Electronic Supplementary Material (ESI) for MedChemComm.

Supporting information

Structure Activity Relationship of 2-Arylalkynyl-adenine Derivatives as Human A_3 Adenosine Receptor Antagonists

Jinha Yu, Philip Mannes, Young-Hwan Jung, Antonella Ciancetta, Amelia Bitant, David Lieberman, Sami Khaznadar, John A. Auchampach, Zhan-Guo Gao, and Kenneth A. Jacobson

Contents Pages

Off-target activity, determined by the the Psychoactive Drug Screening Program (PDSP)

Unless noted in the text, no significant interactions (<50% inhibition at 10 μM) for any of the adenine derivatives (**15-29**) were found at the following sites (human unless noted): $5HT_{1A}$, $5HT_{1B}$, $5HT_{1D}$, $5HT_{1E}$, $5HT_{2A}$, $5HT_{2B}$, $5HT_{2C}$, $5HT_3$, $5HT_{5A}$, $5HT_6$, $5HT_7$, α_{1A}, α_{1B}, α_{1D}, α_{2A}, α_{2B}, α_{2C}, β_1, β_2, β_3, BZP rat brain site, D_1, D_2, D_3, D_4, D_5, delta opioid receptor (DOR), $GABA_A$, H_1, H_2, H_3, H_4, M_1, M_2, M_5, mu opioid receptor (MOR), σ_1, σ_2, DAT, NET, SERT. Representative curves are shown.

σ_2 binding of **13** MRS5776 (PDSP 44260)

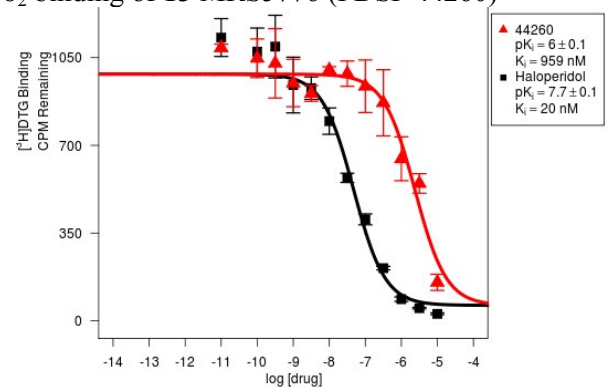

σ_1 binding of **16** MRS7496 (PDSP 52190)

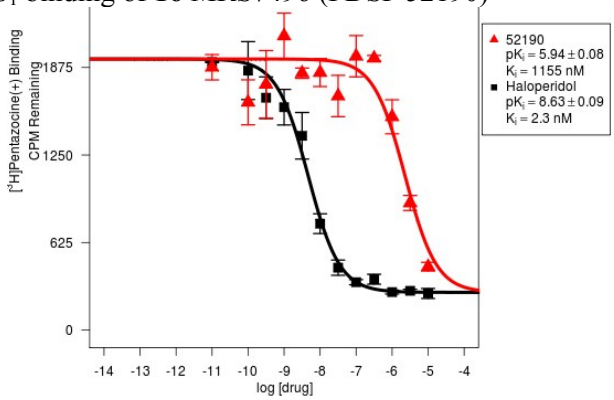

NET binding of **13** MRS5776 (PDSP 44260)

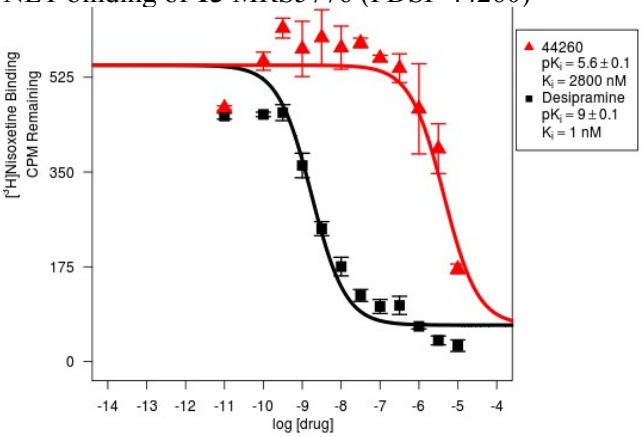

σ_1 binding of **17** MRS7497 (PDSP 52191)

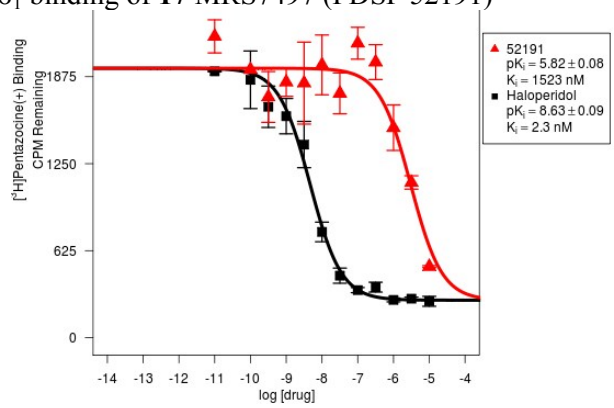

D_1 binding of **16** MRS7496 (PDSP 52190)

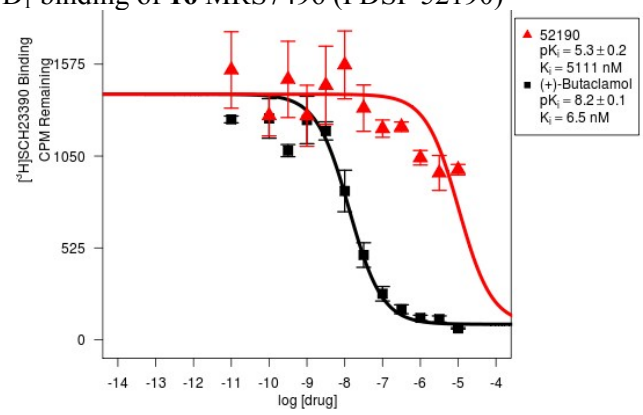

σ_2 binding of **17** MRS7497 (PDSP 52191)

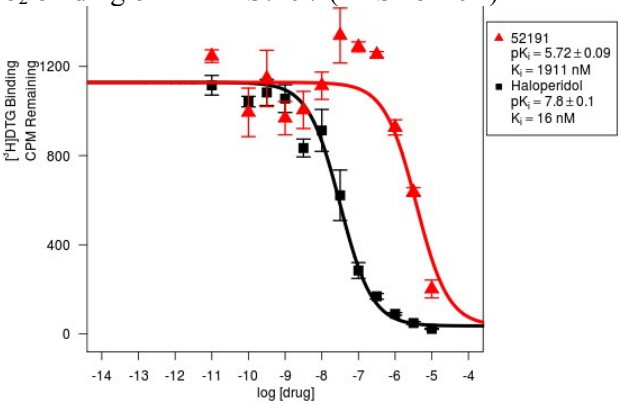

α_{2C} binding of **18** MRS7302 (PDSP 44182)

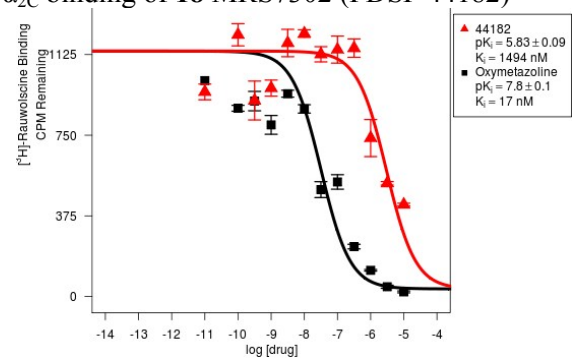

M_4 binding of **20** MRS7324 (PDSP 44183)

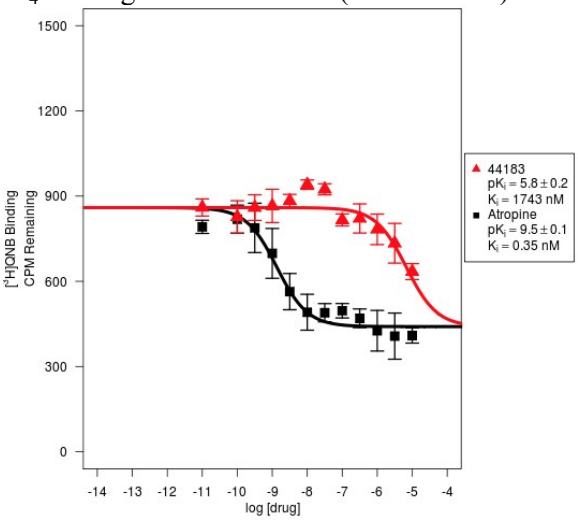

$5HT_{2B}$ binding of **19** MRS7326 (PDSP 44185)

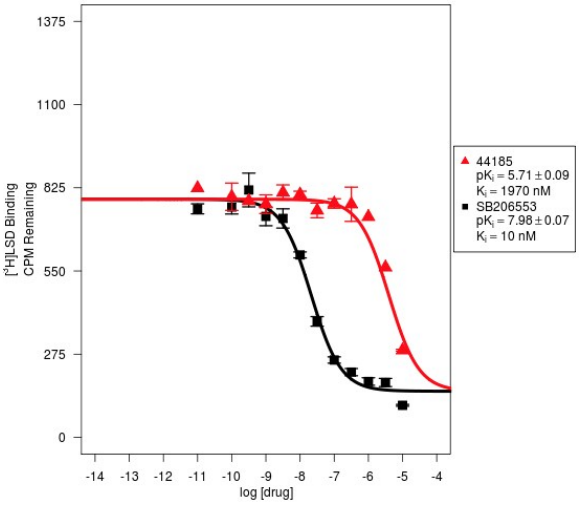

H_2 binding of **21** MRS7351 (PDSP 44965)

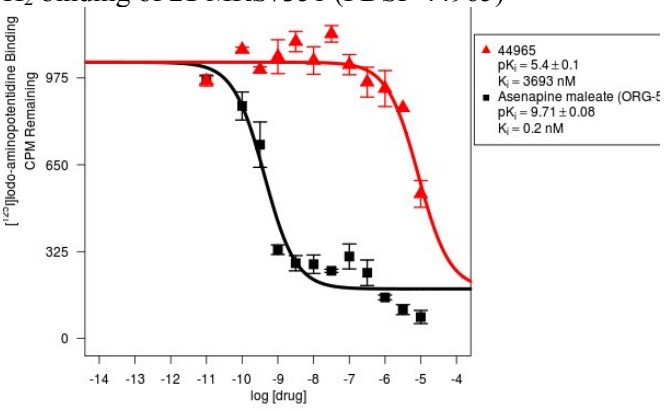

$5HT_{2C}$ binding of **19** MRS7326 (PDSP 44185)

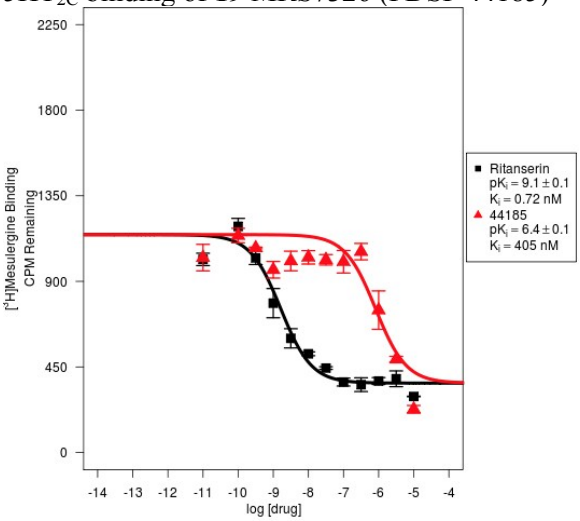

TSPO binding of **22** MRS7325 (PDSP 44184)

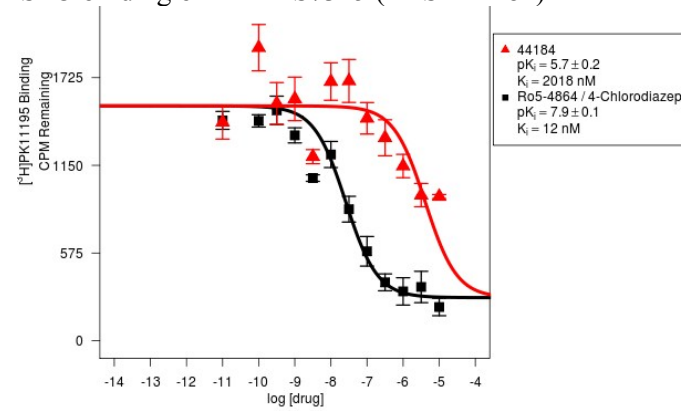

α_{2B} binding of **23** MRS7327 (PDSP 44186)

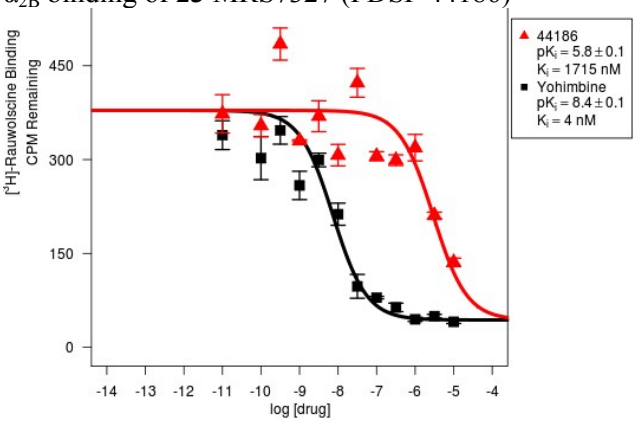

H_2 binding of **24** MRS7350 (PDSP 44964)

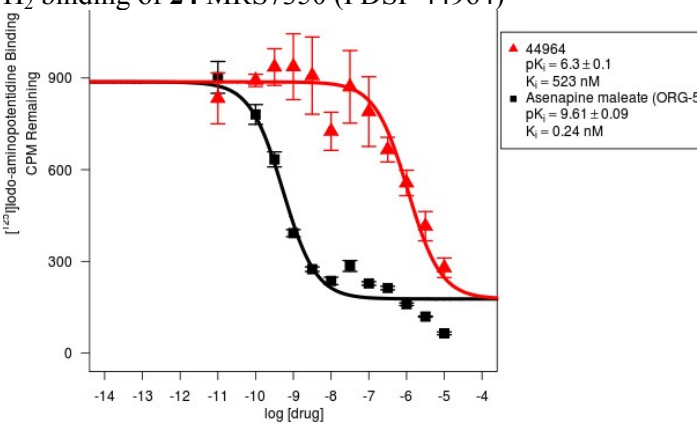

σ_2 binding of **23** MRS7327 (PDSP 44186)

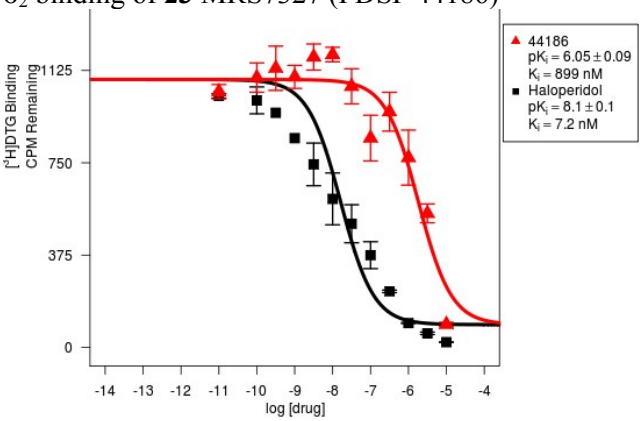

α_{2C} binding of **25** MRS7320 (PDSP 44963)

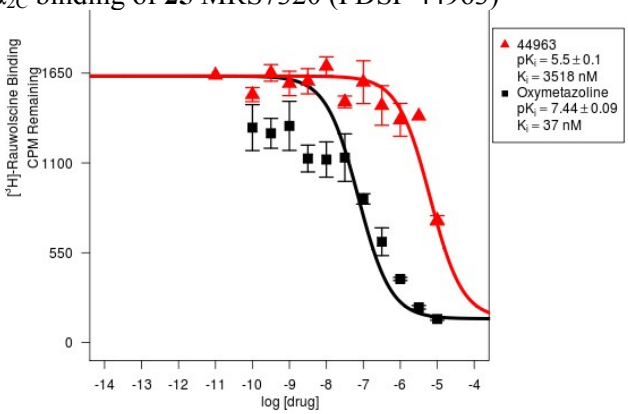

$5HT_{2C}$ binding of **24** MRS7350 (PDSP 44964)

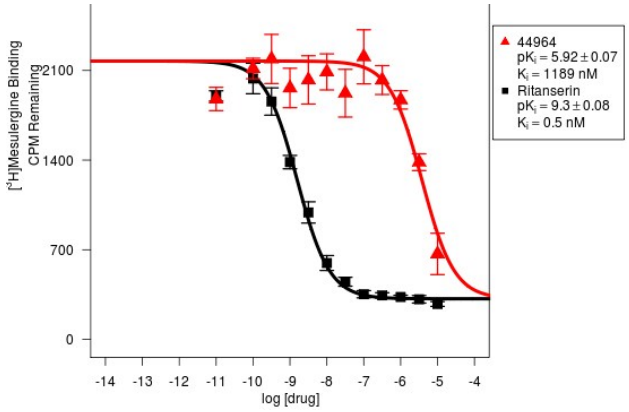

$5HT_{2B}$ binding of **25** MRS7320 (PDSP 44963)

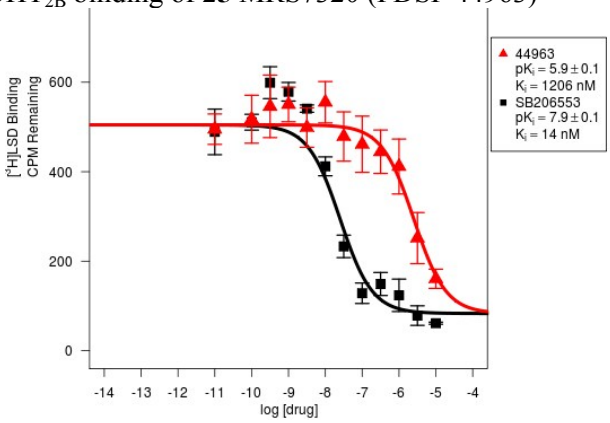

σ_1 binding of **26** MRS7434 (PDSP 52192)

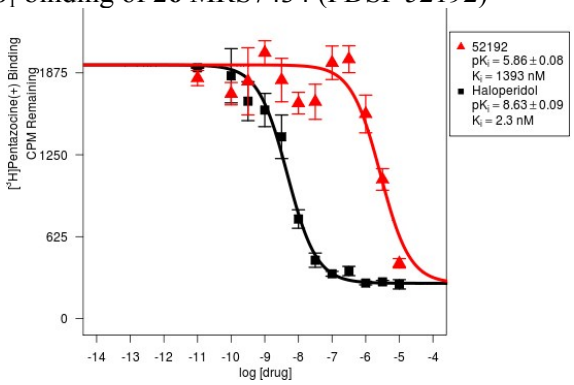

TSPO (r) binding of **27** MRS7398 (PDSP 45541)

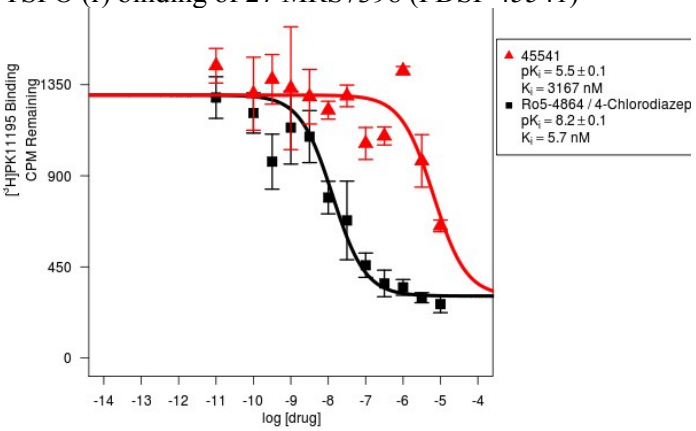

σ_2 binding of **26** MRS7434 (PDSP 52192)

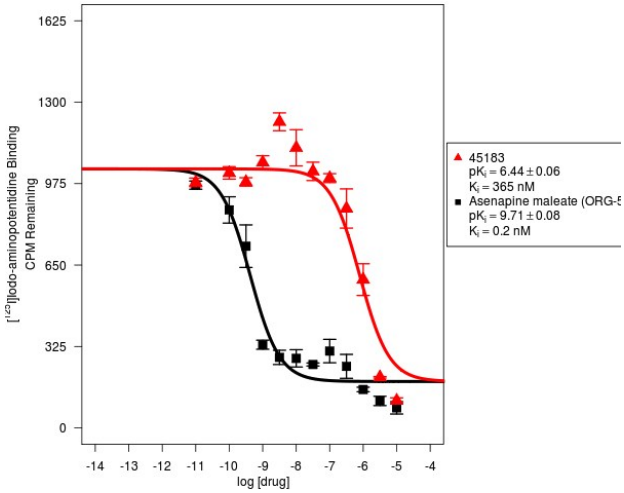

Molecular Modeling

Protein Preparation. A previously build human (h) A_3AR homology model[1] based on the high-resolution inactive $A_{2A}AR$[2] (PDB ID: 4EIY) was used. The protonation state of histidine residues was determined according to H-bond patterns with surrounding residues as follows: His272 and His79/95/124/158 were protonated on the N^{δ} and the N^{ε}, respectively.

Ligand Docking. The ligands (**10**,**15**-**28**) were built using Maestro[3] and docked using Glide search algorithm[4] and OPLS3 force field. Residues Asn250 (6.55), Phe168 (EL2), Tyr265(7.36), and His272 (7.43) were selected as the center of the grid with a box size of 20 Å. Up to 10 poses per ligand were collected using the SP scoring function.

Molecular Dynamics. MD system setup, equilibration, and production were performed with the HTMD[5] module (Acellera, Barcelona Spain, version 1.11.10). The ligand-protein complexes were embedded into an 80 x 80 Å 1-palmitoyl-2-oleoyl-sn-glycero-3-phosphocholine (POPC) membrane leaflet generated through the VMD Membrane Plugin tool. Overlapping lipids (within 0.6 Å) were removed upon protein insertion and the systems were solvated with TIP3P[6] water and neutralized by Na^+/Cl^- counter-ions (final concentration 0.154 M). MD simulations with periodic boundaries conditions were carried out with ACEMD (Acellera, version 2017.11.30)[7] using the CHARMM36[8,9]/CGenFF(3.0.1)[10,11] force fields for lipid and protein, and ligand atoms, respectively. Ligand parameters were retrieved from the ParamChem service (https://cgenff.paramchem.org, accessed 03/2018, version 1.0.0). The systems were equilibrated through a 5000-step minimization followed by 40 ns of MD simulation in the NPT ensemble by applying initial constrains (0.8 for the ligand atoms, 0.85 for alpha carbon atoms, and 0.4 for the other protein atoms) that were linearly reduced after 20 ns. During the equilibration procedure, the temperature was maintained at 310 K using a Langevin thermostat with a low damping constant of 1 ps^{-1}, and the pressure was maintained at 1 atm using a Berendensen barostat. Bond lengths involving hydrogen atoms were constrained using the MSHAKE[12] algorithm. The equilibrated system was subjected to 30 ns of unrestrained MD simulation run in triplicate (NVT ensemble, timestep = 2 fs, damping constant = 0.1 ps^{-1}). Long range Coulomb interactions were handled using the particle mesh Ewald summation method (PME)[13] with grid size rounded to the approximate integer value of cell wall dimensions. A non-bonded cutoff distance of 9 Å with a switching distance of 7.5 Å was used. All simulations were run on two NVIDIA GeForce GTX 970 and 1080.

Trajectory Analysis. MD Trajectories were visually inspected and analyzed using VMD[14] v1.9.3. Ligand root-mean-square deviation and fluctuation (RMSD and RMSF, respectively) and protein alpha carbon atoms RMSD with respect to the initial frame in the production runs were computed with the RMSD trajectory tool (RSMDTT) implemented in VMD.

Modeling References

(1) Ciancetta, A.; Rubio, P.; Lieberman, D.; Jacobson, K. A. A_3 adenosine receptor activation mechanisms predicted using molecular dynamics analysis of inactive, active, and fully active states. Abstract 26, p. 189, Abstracts of Purines2018 International, held in Foz do Igauçu, Brazil, June 19-22, 2018.
(2) Liu, W.; Chun, E.; Thompson, A. A.; Chubukov, P.; Xu, F.; Katritch, V.; Han, G. W.; Roth, C. B.; Heitman, L. H.; IJzerman, A. P.; Cherezov, V.; Stevens, R. C. *Science*, **2012**, *337*, 232–236.
(3) Schrödinger Release 2017-3: Maestro, Schrödinger, LLC, New York, NY, 2017.

(4) Schrödinger Release 2017-3: Glide, Schrödinger, LLC, New York, NY, 2017.
(5) Doerr, S.; Harvey, M. J.; Noé, F.; De Fabritiis, G. HTMD: High-Throughput Molecular Dynamics for Molecular Discovery. *J. Chem. Theory Comput.*, **2016**, *12*, 1845-1852.
(6) Jorgensen, W. L.; Chandrasekhar, J.; Madura, J. D.; Impey, R. W.; Klein, M. L. Comparison of simple potential functions for simulating liquid water. *J. Chem. Phys.* **1983**, *79*, 926−935.
(7) Harvey, M.; Giupponi, G.; De Fabritiis, G. ACEMD: Accelerated molecular dynamics simulations in the microseconds timescale. *J. Chem. Theory Comput.* **2009**, *5*, 1632−1639.
(8) Best, R. B.; Zhu, X.; Shim, J.; Lopes, P. E. M.; Mittal, J.; Feig, M.; MacKerell Jr., A. D. Optimization of the additive CHARMM all-atom protein force field targeting improved sampling of the backbone phi, psi and side-chain chi1 and chi2 dihedral angles. *J. Chem. Theory Comput.* **2012**, *8*, 3257–3273.
(9) Klauda, J. B.; Venable, R. M.; Freites, J. A.; O'Connor, J. W.; Tobias, D. J.; Mondragon-Ramirez, C.; Vorobyov, I.; MacKerell Jr., A. D.; Pastor, R. W. Update of the CHARMM all-atom additive force field for lipids: validation on six lipid types. *J. Phys. Chem. B*, **2010**, *114*, 7830-7843.
(10) Vanommeslaeghe, K.; MacKerell, A. D., Jr., Automation of the CHARMM General Force Field (CGenFF) I: bond perception and atom typing. *J. Chem. Inf. Model.* **2012,** *52*, 3144-3154.
(11) Vanommeslaeghe, K.; Raman, E. P.; MacKerell, A. D., Jr., Automation of the CHARMM General Force Field (CGenFF) II: assignment of bonded parameters and partial atomic charges. *J. Chem. Inf. Model.* **2012,** *52*, 3155-3168.10-13 CHARMM/CGenFF
(12) Kräutler, V.; Van Gunsteren, W. F.; Hünenberger, P. H. A Fast SHAKE algorithm to solve distance constraint equations for small molecules in molecular dynamics simulations. *J. Comput. Chem.* **2001**, *22*, 501−508.
(13) Essmann, U.; Perera, L.; Berkowitz, M. L.; Darden, T.; Lee, H.; Pedersen, L. G. A. Smooth particle mesh Ewald method. *J. Chem. Phys.* **1995**, *103*, 8577−8593.
(14) Humphrey, W.; Dalke, A.; Schulten, K. VMD - Visual molecular dynamics. *J. Mol. Graphics* **1996**, *14*, 33−38.

Table S1. Parameter considered for the selection of a representative trajectory among three replicas: ligand average root-mean-square deviation (RMSD) with respect to the first frame. Values are in Å. The run selected for visualization (Video S1) is marked in bold.

Initial Docking Pose	Run Number	Average Ligand RMSD [Å]
17 (BM1)	Run1	2.12±0.63
	Run2	**1.76±0.42**
	Run3	1.50±0.50
17 (BM2)	Run1	6.11±3.50
	Run2	3.17±0.84
	Run3	2.92±0.98

Figure S1. Superimposition of the docking poses of the adenine antagonist **17** (magenta carbon sticks) and the adenosine agonist **10** (green carbon sticks) at the hA_3AR inactive homology model (grey carbon lines). H-bond and π-π interactions are depicted as yellow and cyan dashed lines, respectively.

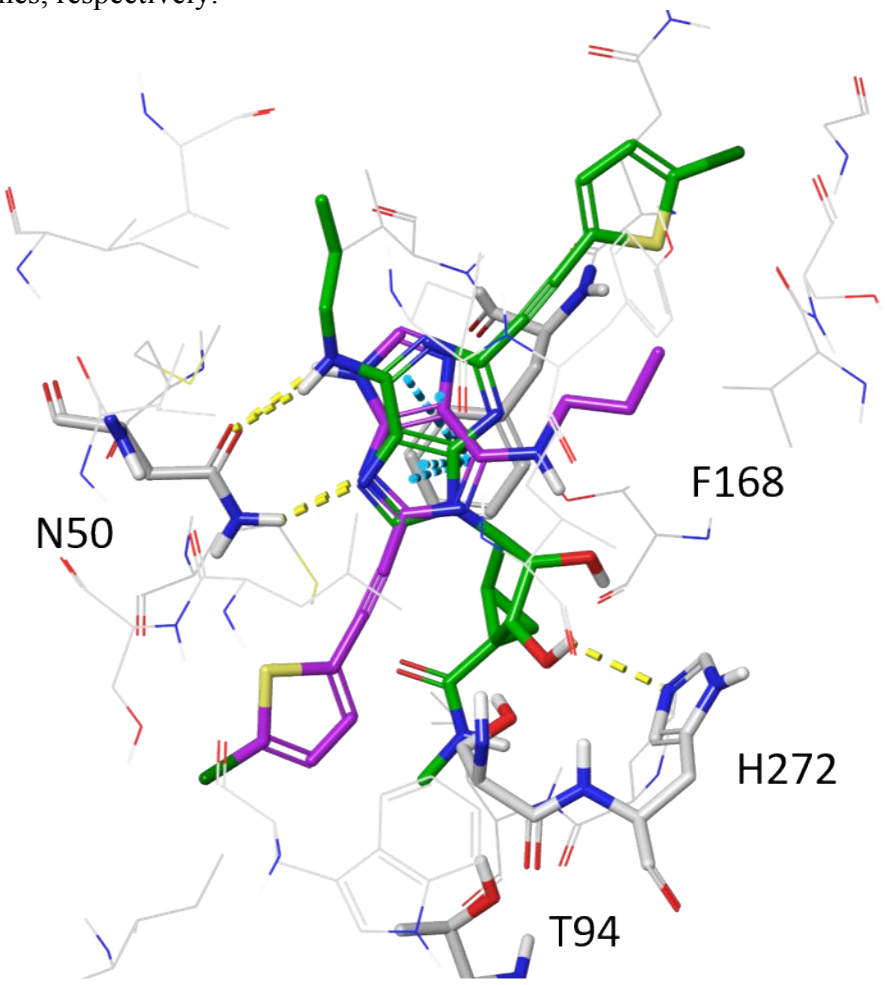

Figure S2. BM2 of **17** was generated by removing the N-methanocarba ring (red cross) from the docking pose of the agonist **10**.